Supplementary Information

Materials and Methods:

Cell culture and treatments. IMCD3 cells were maintained in DMEM-F12 supplemented with 10% calf serum. Starvation and cilium assembly were achieved by 24/48 hrs of serum deprivation. IMCD3 at 80% confluency were transfected on coverslips in 24-well plates with 0.5 µg of plasmid DNA using the Effectene Transfection Reagent (Qiagen, Hilden, Germany). GFP- and GFP- Rab8a^{Q67L} IMCD3 stable cell lines were obtained by Geneticin selection. Briefly, IMCD3 cells were plated in 12-well plates and transfected with either EGFP-C3 or GFP- Rab8a^{Q67L} plasmid. After 36 hours, cells were plated in a 9 cm plate and medium was replaced with medium containing Geneticin G418 Sulphate (Life Technologies). Resistant cells were then plated at single cell dilution to allow clonal selection of GFP-positive clones.

Immunofluorescence. Immunofluorescence of PFA 4% fixed IMCD3 cells followed standard procedures. Raw images were digitally processed only to normalize the background and enhance the contrast. Cells were stained with DAPI and examined with either Leica TCS-II SP5 confocal microscope, or a Zeiss Observer-Z1 microscope, equipped with Apotome. Z-stacks were acquired and processed with the Maximum Projection tool. 3D morphometric measurement of ciliary length was performed with Filament tool of Imaris (BitPlane, Zurich, Switzerland). In situ localization of Polycystin-2 and acetylated-Tubulin in nodal cilia was done on embryos at the presomite stage essentially as described in [1]. Primary antibodies: anti-Acetylated-Tubulin monoclonal (6-11B-1, Sigma, St. Louis MO, USA), anti-Acetylated-Tubulin polyclonal D20G3 (Cell Signaling Technology, Boston, MA, USA), anti-PI3K-C2α monoclonal (anti p170 #611046 BD Transduction Laboratories), anti-Rab11a polyclonal (Abcam, Inc Cambridge MA), anti-Polycystin2 D3 monoclonal (Santa Cruz Biotechnology, Santa Cruz, CA, USA). Secondary antibodies were: goat anti-rabbit and goat anti-mouse, labelled with Alexa-488 or -568 (Molecular Probes/Invitrogen).

Scanning Electron Microscopy. Samples were fixed ON at 4°C in 2.5% glutaraldehyde, 0.1M cacodylate buffer (pH 7.2) and post-fixed in 2% OsO 4 in the same buffer. After serial dehydration in increasing ethanol concentrations, samples were dried at critical point,

coated with platinum by standard procedures, and examined in a ESEM Tecnai Quanta 200 FEG (FEI).

Histological Analyses and Immunohistochemistry. Kidneys were isolated and fixed overnight with paraformaldehyde 4%. Samples were dehydrated, paraffin embedded and sectioned into 3 µm thick slices. Standard protocols where followed for the quantification of tubular dilations [2]. Briefly, cortical sections were stained with Hematoxylin-Eosin, three 20x fields/kidney were photographed and the TD/cystic index was calculated: a grid composed of 13,6 µm-spaced dots was overlapped on the images, the tubules were counted/scored according to the number of dots present in their lumen (Tubular dilation, 2 dots; microcysts, 3-9 dots; Cyst, >9 dots). To visualize extracellular matrix deposition, sections were stained with Picrosirius red (Fluka, Buchs, Switzerland). The percentage of fibrosis (red staining) over the total tissue was calculated by Metamorph software (Universal Imaging Corporation, Downingtown, PA, USA). 5 fields were quantified for each kidney. For immunohistochemical analyses rabbit monoclonal antibodies against pErk1/2 (Phospho-p44/42 MAPK Thr202/Tyr204, Cell Signaling #4376) and pS6rp (Phospho S6Rp Ser240/244, Cell Signaling #2217) were used on paraffin sections. Rabbit anti-rat IgG (Dako Cytomation, Milano, Italy) was used as the biotinylated secondary antibody. PCNA staining was performed using mouse monoclonal antibodies against PCNA (SantaCruz Biotechnology,) and the Vector M.O.M. Immunodetection Kit (Vector Laboratories, Burlingame, CA, USA). Immunoreactivity was detected with the streptABCComplex/HRP system (DakoCytomation; Milano, Italy) and developed with DAB (methanol 3,3 diamino-benzide, Roche Diagnostic Corp., Milano, Italy). Sections were analyzed on an Olympus BX41 microscope (objective Olympus Plan 4X, 10X or 40X) equipped with an Olympus DP50 camera for images acquisition (Olympus, Milan, Italy). For quantifications, 5 fields were analysed for each kidney.

Western blotting. Protein extraction, SDS-PAGE and western blotting followed standard procedures. Antibodies: anti-PI3K-C2α monoclonal (anti p170 #611046 BD Transduction Laboratories), anti-Rab11a monoclonal (BD Bioscience #610657), anti-phosphoS6K polyclonal (Phospho-p70 S6 Kinase (Thr389) Cell Signaling #9205), anti-S6K polyclonal (p70 S6 kinase α (C-18) sc-230), anti-phosphoS6 polyclonal (Phospho-S6 Ribosomal Protein (Ser235/236) Cell Signaling #2211), anti-phosphoERK polyclonal (Phospho-p44/42 MAPK (Erk1/2)(Thr202/Tyr204) Cell Signaling #9101), anti-ERK polyclonal (p44/42 MAPK (Erk1/2) Cell Signaling #9102), anti-p21 monoclonal (P21 (F-5) sc-6246 Santa Cruz), anti-

phosphoCREB monoclonal (Phospho-CREB (Ser133) Cell Signaling #9198). Anti-GFP and Anti-Vinculin are homemade produced.

References:

1. Franco, I, Gulluni, F, Campa, CC, Costa, C, Margaria, JP, Ciraolo, E, Martini, M, Monteyne, D, De Luca, E, Germena, G, Posor, Y, Maffucci, T, Marengo, S, Haucke, V, Falasca, M, Perez-Morga, D, Boletta, A, Merlo, GR, Hirsch, E: PI3K Class II alpha Controls Spatially Restricted Endosomal PtdIns3P and Rab11 Activation to Promote Primary Cilium Function. Dev Cell, 28: 647-658, 2014.

2. Bastos, AP, Piontek, K, Silva, AM, Martini, D, Menezes, LF, Fonseca, JM, Fonseca, II, Germino, GG, Onuchic, LF: Pkd1 haploinsufficiency increases renal damage and induces microcyst formation following ischemia/reperfusion. J Am Soc Nephrol, 20: 2389-2402, 2009.

Supplementary Figures:

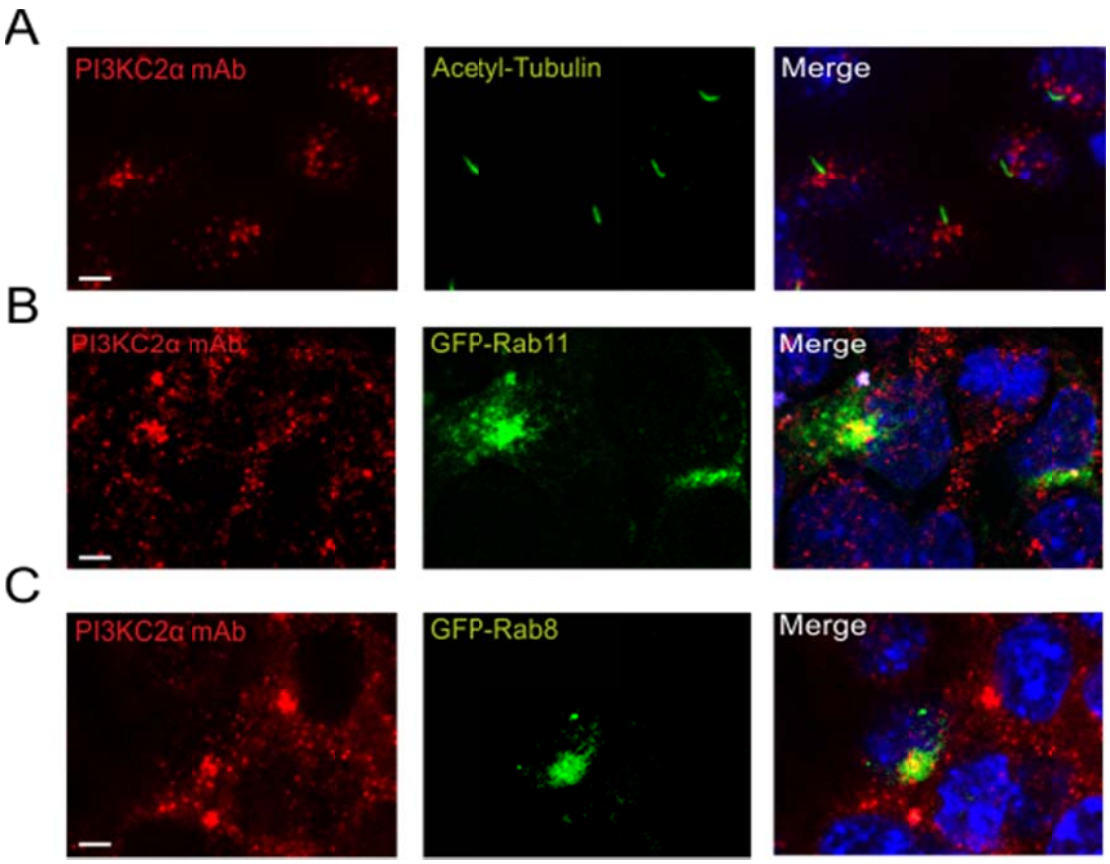

Supplemental Figure 1. PI3K-C2α localizes around the base of the primary cilium. (A) Immunofluorescence analysis of control-IMCD3 cells stained with anti-PI3KC2α antibody (red). Cilium (green) and nuclei (blue) staining is provided. Bar= 3μm. (B-C) Confocal images of control-IMCD3 cells transfected with either GFP-Rab11 (B) or GFP-Rab8 (C) and stained with anti-PI3KC2α antibody (red), show partial co-localization of PI3KC2α with these markers of the pericentriolar recycling endosome. Bar= 3μm.

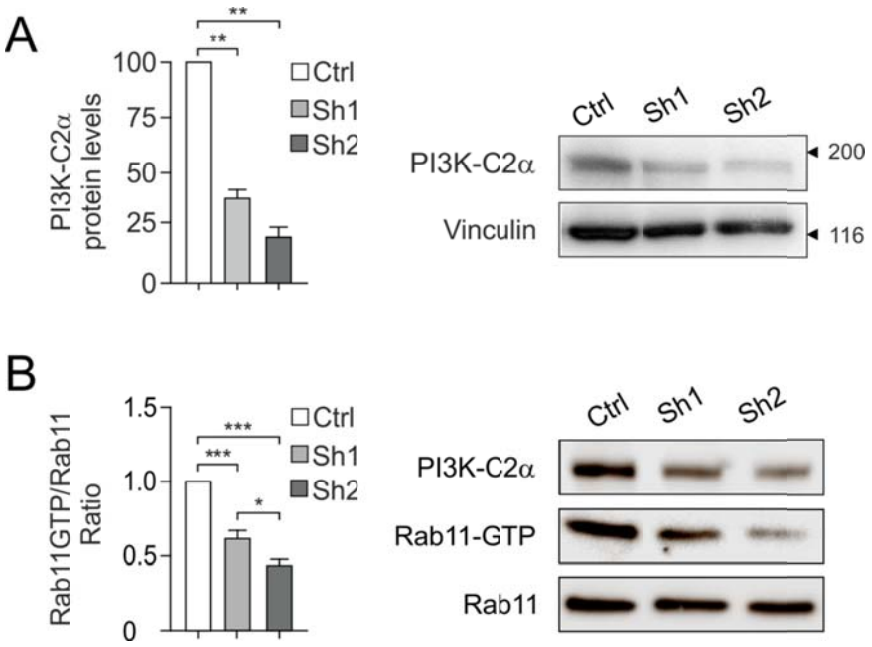

Supplemental Figure 2. PI3K-C2α regulates Rab11 activation in a dose dependent manner in IMCD3 cells. (A) Western blot analysis with anti-PI3K-C2α antibody in IMDC3 cells infected with either a control sequence (empty-pGIPZ) or shRNAs downmodulating PI3K-C2α (Sh1 and Sh2). Different efficiency of silencing produced two cell lines showing 40% (Sh1) or 20% (Sh2) PI3K-C2α levels of control cells. (B) Pull down experiment showing the endogenous content of Rab11-GTP in IMCD3 cells downmodulated for PI3K-C2α (Sh1 and Sh2). Lower levels of PI3K-C2α (Sh2) corresponded to more severe impairment of Rab11 activation. N=6 independent experiments.

A

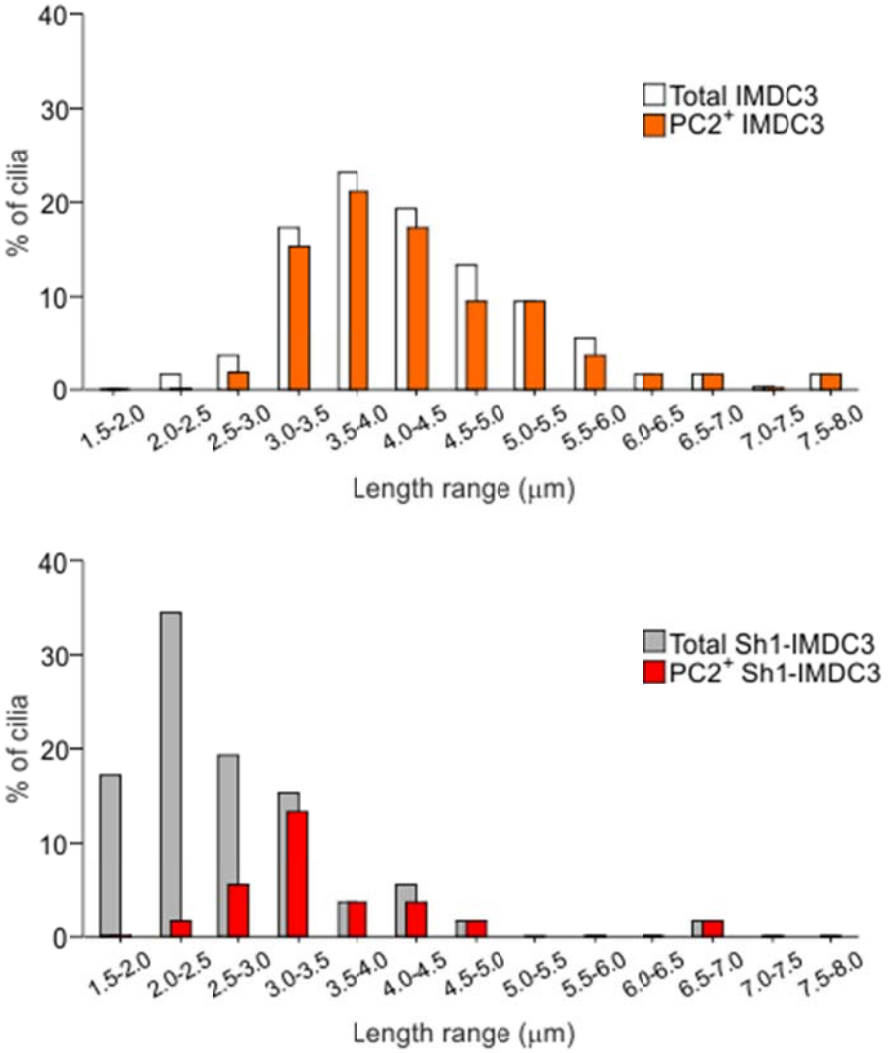
40
30
20
10
0
% of cilia
Total IMDC3
PC2+ IMDC3
1.5-2.0
2.0-2.5
2.5-3.0
3.0-3.5
3.5-4.0
4.0-4.5
4.5-5.0
5.0-5.5
5.5-6.0
6.0-6.5
6.5-7.0
7.0-7.5
7.5-8.0
Length range (μm)
40
30
20
10
0
% of cilia
Total Sh1-IMDC3
PC2+ Sh1-IMDC3
1.5-2.0
2.0-2.5
2.5-3.0
3.0-3.5
3.5-4.0
4.0-4.5
4.5-5.0
5.0-5.5
5.5-6.0
6.0-6.5
6.5-7.0
7.0-7.5
7.5-8.0
Length range (μm)

B

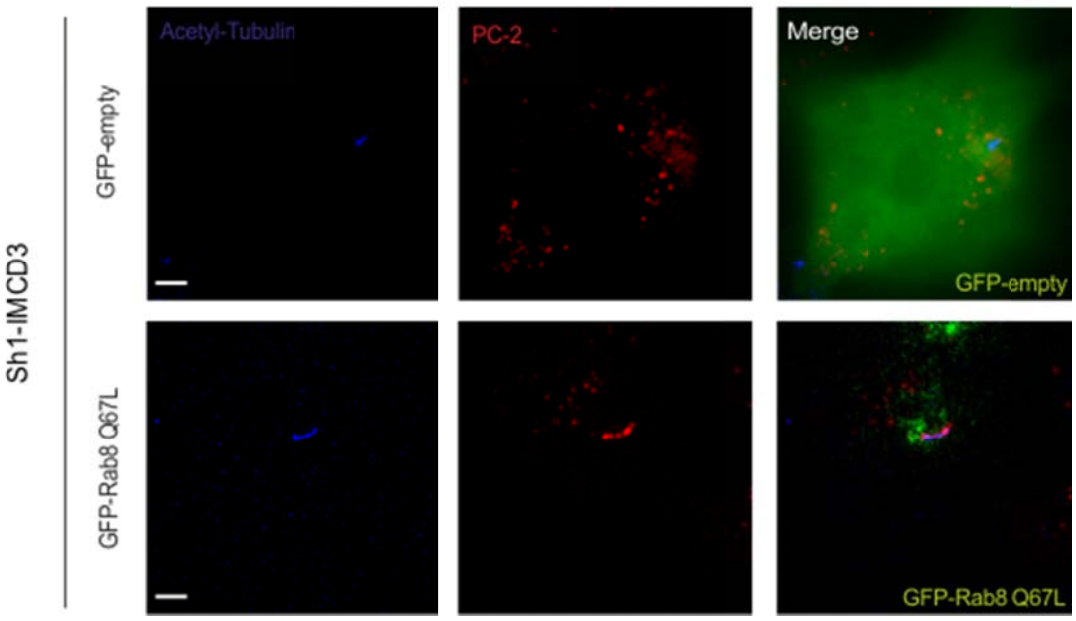
Sh1-IMCD3
GFP-empty
GFP-Rab8 Q67L
Acetyl-Tubulin
PC-2
Merge
GFP-empty
GFP-Rab8 Q67L

Supplemental Figure 3. (A) Measurement of ciliary length and Polycystin-2 positive staining, obtained in parallel for each primary cilia (n=50 cilia for each condition), analysing wild-type (IMCD3) or Sh1-treated IMCD3 (Sh1-IMCD3) cells after 48-hour starvation. Percent frequency of cilia in a specific length range (Total) is shown superimposed to percent frequency of Polycystin-2 positive cilia in the same length range ($PC2^{+}$). (B) Rescue of Polycystin-2 ciliary localization by transfection of constitutively active Rab8. Representative immunofluorescence of Polycystin-2 (PC2, red) on cilia (acetilated-α-tubulin, blue) of 48 hours-starved Sh1-IMCD3 cells, after transfection with either a control plasmid (empty-EGFP, green, upper panels) or constitutively active Rab8 (GFP-$Rab8^{Q67L}$, green, lower panels). Sh1-IMCD3 cells transfected with the control plasmid show a defective accumulation of PC2 on cilia, while the transfection of GFP-$Rab8^{Q67L}$ rescues this defect. Bar= 3 μm.

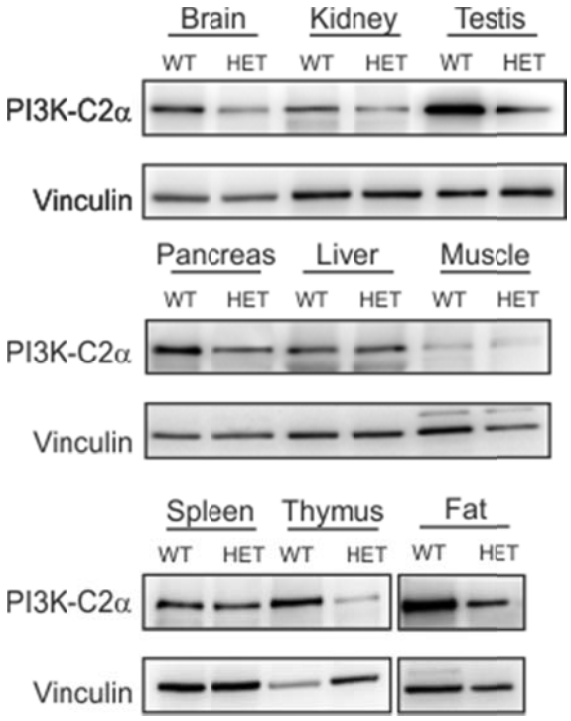

Supplemental Figure 4. Analysis of *Pik3c2a*$^{+/-}$ adult mice. Western blot analysis of PI3K-C2α protein levels in wild-type and *Pik3c2a*$^{+/-}$ adult tissues. Equal loading was monitored by vinculin. Reduction of PI3K-C2α protein levels is observed in most heterozygous tissues including the kidney (first row).

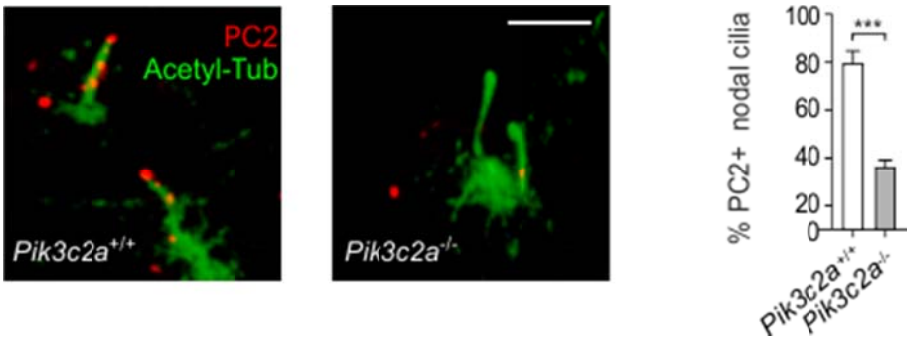

Supplemental Figure 5. Polycystin-2 fails to localize to ventral node cilia in *Pik3c2a*$^{-/-}$ embryos. Whole mount immunofluorescence of wild-type and *Pik3c2a*$^{-/-}$ embryos at the early somite stage. Cilia of the ventral node were stained for PC2 (red) and acetyl-tubulin (green) and the percentage of PC2 positive cilia was calculated in n=3 wild type and n=3 *Pik3c2a*$^{-/-}$ embryos.

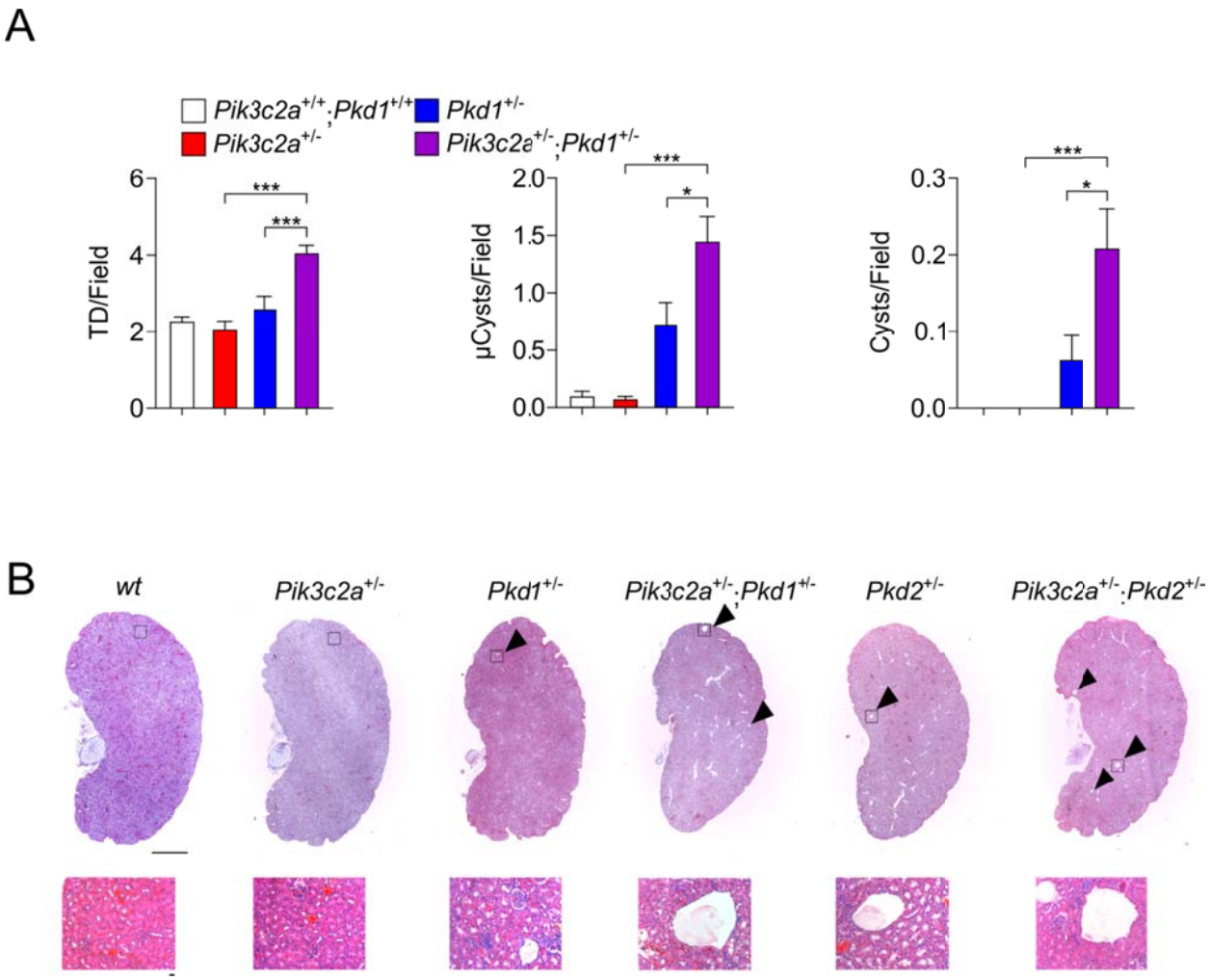

Supplemental Figure 6. Heterozygous loss of *Pik3c2a* enhances cysts formation in Polycystin-1 and 2 heterozygous mutants. (A) Quantification, using the TD/cysts index, of tubular dilations (TD, left), microcysts (µCysts, middle) and cysts (right) observed in n=10 wild type, n=11 *Pik3c2a*$^{+/-}$, n=8 *Pkd1*$^{+/-}$ and n=12 double heterozygotes *Pik3c2a*$^{+/-}$;*Pkd1*$^{+/-}$ outbred mice. 3-months old mice were analysed. (B) Representative low magnification images (2X) from Hematoxylin/eosin stained whole kidneys (top) with the specified genotypes; boxed regions are enlarged in the bottom panel. Arrowheads indicate cysts. Scale bars, 1 mm (top); 13.6 µm (bottom).

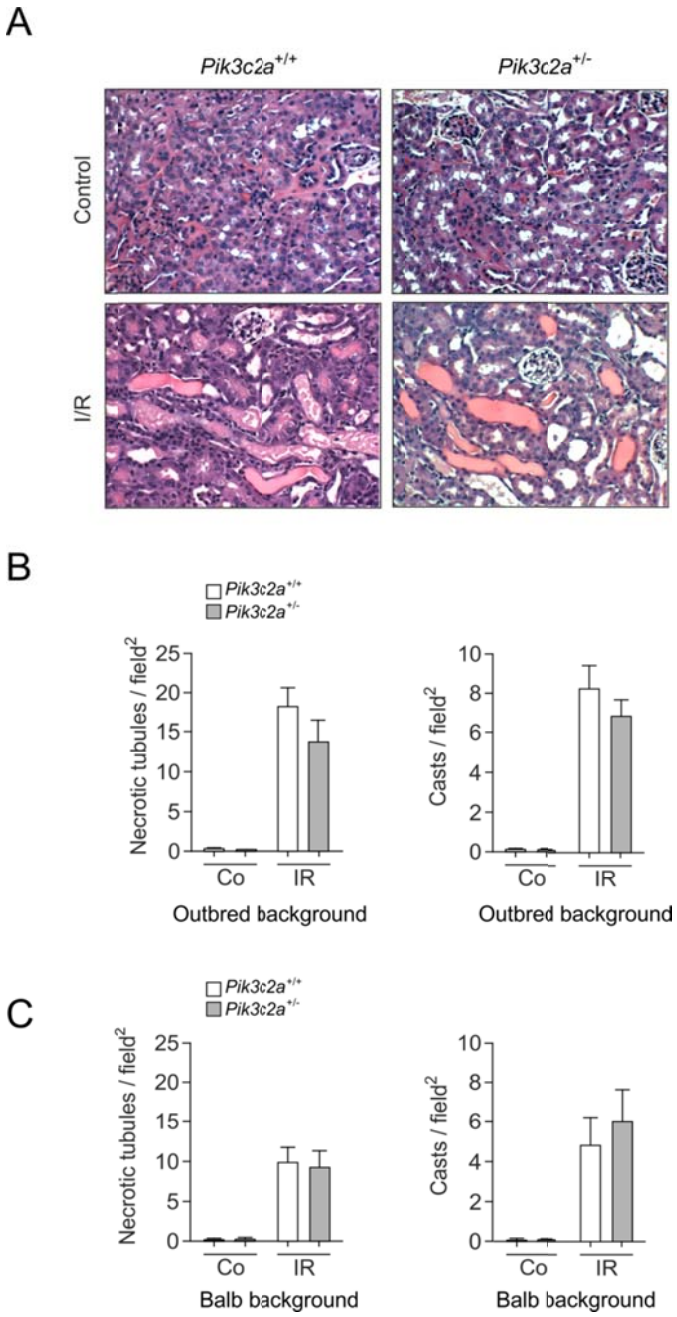

Supplemental Figure 7. I/R-induced tubular necrosis at 48 hours after treatment. (A) Hematoxylin/eosin staining of wild-type (left) and *Pik3c2a*$^{+/-}$ (right) outbred kidneys, either untreated (Control) or subjected to Ischemia/Reperfusion (I/R) followed by a 48 hours recovery. Bar=100 µm. (B-C) Quantification of necrotic tubules and casts in wild-type and *Pik3c2a*$^{+/-}$ kidneys in either outbred (B) or inbred BALB/c (C) background.

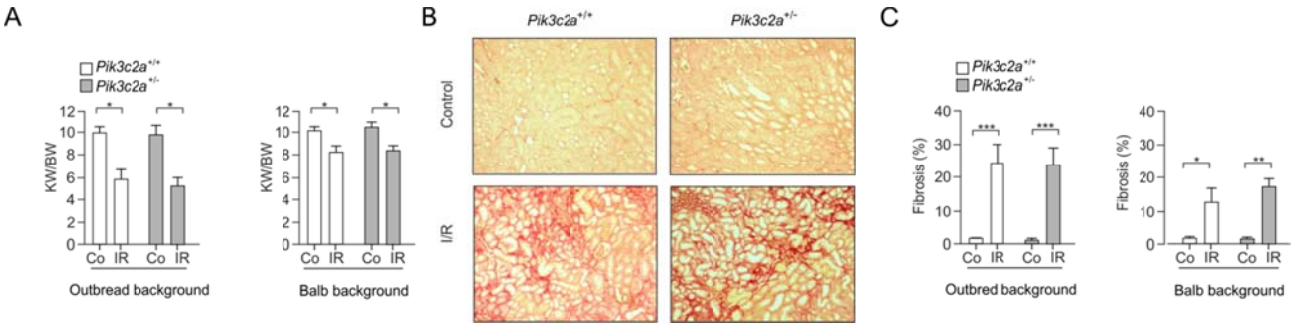

Supplemental Figure 8. I/R-induced kidney remodelling in *Pik3c2a*$^{+/-}$ mice. (A) Kidney weight loss in wild-type and *Pik3c2a*$^{+/-}$ mice after I/R and 6 weeks recovery. Kidney weight (KW) is normalized on mouse body weight (BW). The left kidney (untreated) of each animal is used as control. While weight reduction of I/R compared to control kidneys is evident in mice of outbred background (leftward graph), BALB/c mice are less sensitive to kidney injury caused by I/R (rightward graph). (B-C) Analysis of kidney fibrosis 6 weeks after I/R. (B) Representative micrographs of Picrosirius red stained kidneys from wild-type (left) and *Pik3c2a*$^{+/-}$ (right) outbred mice. (C) Quantification of the percentage of fibrosis in the kidney tissue of either untreated (Control) or ischemized (I/R) kidneys from wild-type and *Pik3c2a*$^{+/-}$ mice both in the outbred or inbred BALB/c background. n=6, all groups. Bar=100 µm

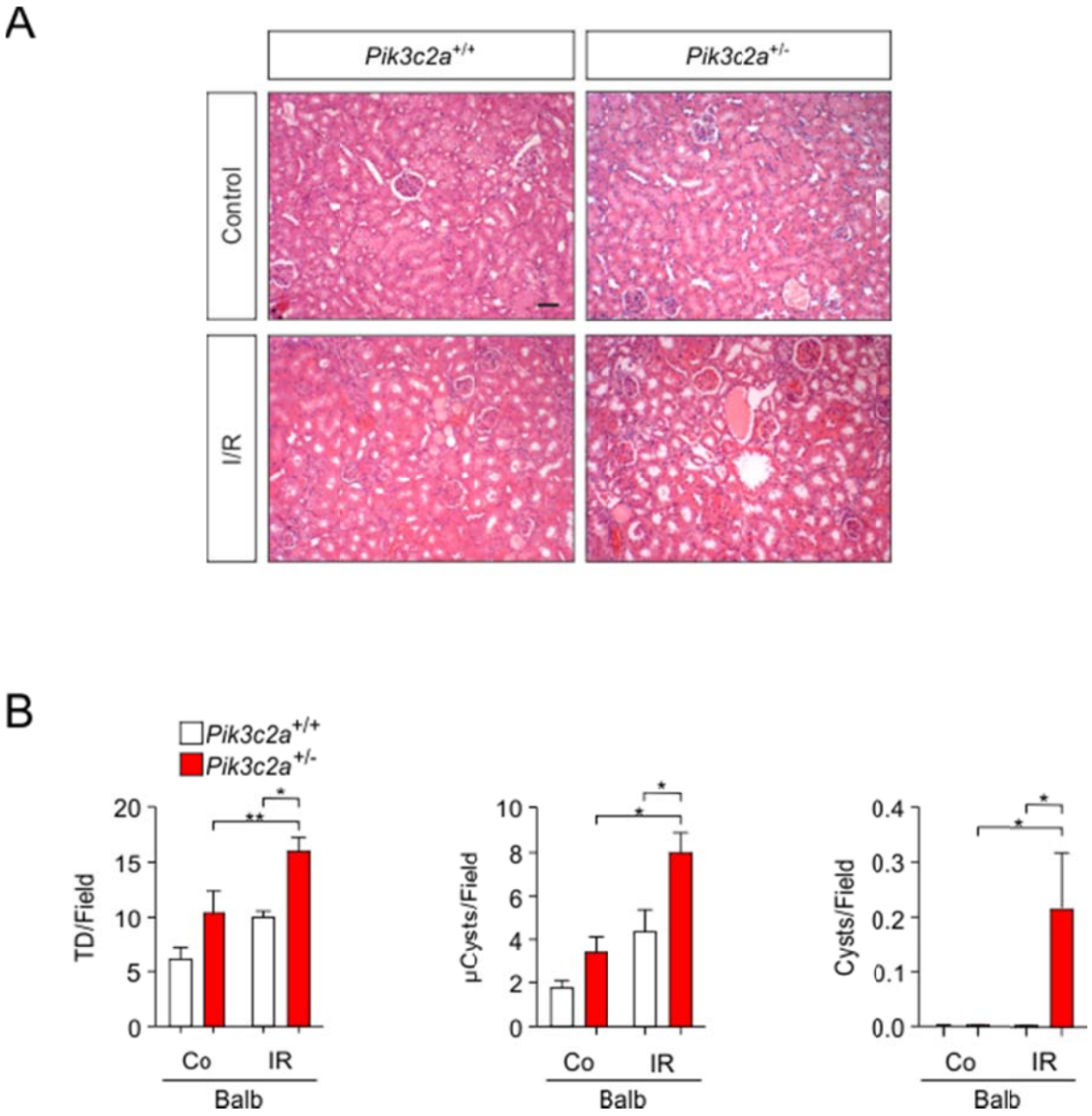

Supplemental Figure 9. I/R-induced tubular dilations in *Pik3c2a*$^{+/-}$ mice at 6 weeks after treatment. (A) Low magnification images from Hematoxylin/eosin stained sections of wild-type (left) and (right) outbred kidneys, either untreated (Control) or subjected to Ischemia/Reperfusion (I/R). A cyst is evident in the section from *Pik3c2a*$^{+/-}$ kidney. Bar=100 µm. (B) Quantification, using the TD/cyst index, of tubular dilations (TD, left), microcysts (µCysts, middle) and cysts (right) in n=8 wild type and n=7 *Pik3c2a*$^{+/-}$ Balb/c mice.

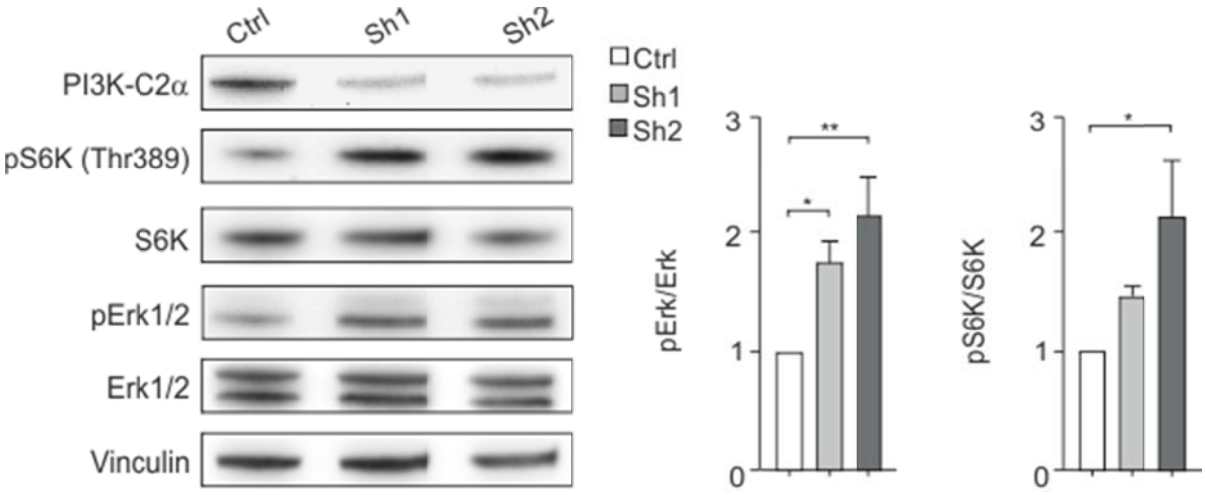

Supplemental Figure 10. PI3K-C2α regulates the activation of proliferative pathways in IMCD3 cells. Western blot analysis of the activation of the MAPK and mTOR pathways in control and *Pik3c2a*-silenced IMCD3 cells (Sh1 and Sh2-IMCD3). A representative western blot showing increased phosphorylation of ERK and p70S6K in Sh1 and Sh2-IMCD3 cells is shown on the left. Protein quantification of n=6 independent experiment is provided on the right.